

Microstructure and fracture behavior of friction stir lap welding of dissimilar AA 6060-T5/ Pure copper

Shubhavardhan Ramadurga Narasimharaju^{a*} and Surendran Sankunny^b

^aDepartment of Mechanical Engineering, University of Saskatchewan, Saskatoon, Canada

^bIndian Institute of Technology, Madras Chennai, India

ARTICLE INFO

Article history:

Received 27 December, 2018

Accepted 18 May 2019

Available online

18 May 2019

Keywords:

Friction stir lap welding

Aluminum

Copper

Interface microstructure

Intermetallic layer

Fracture strength

ABSTRACT

This study aims to understand the uncertainty about the optimum or best pin position (D_p) for friction stir lap welding (FSLW) of Al-Cu. Tensile shear testing is used to determine the Mechanical strength of FSL welds under static loading. Fracture strength (σ_{Lap}) corresponding to the maximum load in a test over the sample width is used as the strength value. Interface microstructures differ depending on whether the tool pin penetrates the lapping interface. It has been found that σ_{Lap} values of the defect free weld samples vary quite significantly and in general are significantly higher than those reported in the literature. When the pin penetration is close to zero no intermetallic layers were formed, hence the value of σ_{Lap} was zero. When the pin penetration is 0.4mm, the commonly observed a thin Al-Cu interface layer forms and this layer does not grow beyond $3\mu m$. It is shown that the thin interfacial layer can withstand a high tensile-shear load and thus the adjacent Al material shears to fracture. When the pin penetrates more than 0.4mm, the commonly observed mix stir zone (MSZ) forms and values of σ_{Lap} are lower than that of 0.4mm pin penetration welds but remain quite high.

© 2019 Growing Science Ltd. All rights reserved.

1. Introduction

Friction stir welding (FSW) is a solid state welding process invented and patented by The Welding Institute (TWI), for butt and lap welding of ferrous and non-ferrous materials and plastics (Thomas et al., 1993). As a good ability of this technique, sound quality weldments for similar Al-Al and dissimilar Al-non Al alloys can be obtained using FSW joining method (Wang et al., 2018; Zhang et al., 2018; Kumbhar & Bhanumurthy, 2012; Lomolino et al., 2005; Torabi et al., 2018; Pao et al., 2001; Zettler et al., 2006; Sun et al., 2013; Aliha et al., 2018; Akbari et al., 2016). In general, it is well known that fusion welding of one metallic alloy to another with considerably higher melting temperatures (referred to as a large ΔT Melting couple, in this case it is Al to Cu) is important in many industries but are very challenging due to physical mismatches such as differences in melting temperature, thermal expansion and thermal conductivity can make the joining almost impractical using conventional welding techniques. Formation of thick intermetallic layers (due to high heat input and liquation of aluminum) is known to deteriorate mechanical properties of the joints (Mishra & Ma, 2005; Mishra & Mahoney, 2007; Nandan et al., 2008; Threadgill et al., 2009; Murr, 2010; Lohwasser & Chen, 2009; Rai et al., 2011). Therefore, development of FSW as a solid-state joining process is of high importance from both scientific

* Corresponding author.

E-mail addresses: shr492@mail.usask.ca (S. Ramadurga Narasimharaju)

and industrial point of view. Fig. 1 illustrates FSLW during which a section of lapping surfaces of the top and bottom plates is stirred and mixed in the stir zone (SZ) thus forming a weld behind the tool. In FS welding of a large ΔT Melting couple, aided by frictional and deformation heat, metallurgical bond is established through diffusion and subsequent formation of interfacial intermetallic. A metallurgical bond is a condition for a quality joint and a metallurgical bond implies low electric resistance, although intermetallic are commonly viewed to affect joint strength adversely. The cited studies on FS Al-to-Cu (including : Galvao et al., 2011, 2012a,b; Elrefaey et al., 2004, 2005; Abdollah-Zadeh et al., 2008; Saeid et al., 2010; Xue et al., 2010, 2011a,b; Satya Narayana Gupta et al., 2012; Firouzdor & Kou, 2012; Akbari & Behnagh, 2012; DebRoy & Bhadeshia, 2010; Ouyang et al., 2006; Aliha et al., 2018, 2019; Esmaili et al., 2011 a,b; Liu et al., 2011; Genevois et al., 2011; Sharma et al., 2018) basically converges on three the general aspects; 1: Al-Cu couple being FS weld able, 2: it is difficult to achieve sound FSW dissimilar Al-Cu joints due to the formation of brittle interfacial intermetallic layer compound (IMCs) at the interface and 3: it is hard to control the formation of IMCs. Early investigation by Elrefaey et al. (2004, 2005) on Al-Cu FSLW clearly established that the tool pin (0.1 and 0.2 mm) penetrating to Cu are the conditions for a metallurgical joint to be established at the Al-Cu interface, resulting in a good joint strength. Although detailed quantification was not done in their study, it was clear from their micrographs that the interface region of welds made with pin penetration is a highly irregular structure of mix layers. Ouyang et al. (2006) attributed the poor weldability to various brittle IMCs formed in the Nugget zone (NZ). It is well documented that several parameters, such as tool offsetting, rotation rate, and traverse speed, influenced the weld properties of the dissimilar Al-Cu FSW joints by Carlone et al. (2015). Abdollah-Zadeh et al. (2008) and Saeid et al. (2010) reported irregular shape and inhomogeneous distribution of IMCs at the interface during FSLW of Al-Cu with minimum pin penetration. Xue et al. (2010, 2011a,b) study was an attempt to correlate the σ_{Lap} to the lower rotation rate and larger bonding area, under the condition of pin penetration. Their data shows that increasing the pin diameter results in a larger Al-Cu bonding area exhibited a higher failure load of 268N/mm with the specimen failing in the HAZ on the aluminium side. However, the meaning of the referred larger bonding area results in wide area intermetallics is unclear and difficult to understand. Furthermore Xue et al. (2011a) reported that Al_4Cu_9 , and Al_2Cu and formed at the interface region, based on x-ray diffraction analysis. However, assigning the structure of Al_4Cu_9 , and Al_2Cu to a mixed region relying on x-ray diffraction analysis is not reliable due to very low intensity. Sharma et al (2018), attributed the effect of different FSW tool pin profiles on the microstructure and the hardness. Firouzdor and Kou (2012) reported weld strength equal to 183 N/mm for conventional Al-Cu FSL weld when the pin penetration at least 0.1mm to Cu. This is a very low weld strength value and from their micrographs a continuous metallurgical bond in Al-Cu interface cannot be confirmed, However, good metallurgical bonding and reasonable tensile properties were ensured when modified lap was used, with increase in weld strength close to 342 N/mm. Satya Narayana Gupta et al. (2012) suggested that better joint properties are obtained in the joints fabricated using straight fluted tool compared with tapered tool and their Micrographs of stir zone are not clear, and Al-Cu interface joint features are not provided. In this paper FSLW of Al-Cu, to explain how interface microstructures affect the fracturing process during tensile-shear testing and thus joint strength. A possible control method for producing Al-Cu welds for a higher joint strength can then be suggested.

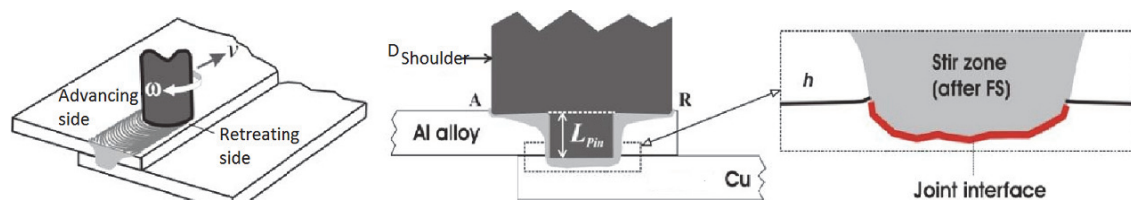


Fig. 1. Schematics illustrations of FSLW of Al-Cu

2. Experimental procedure

All FSLW experiments were conducted using FV200 milling machine and thus the mode of FS was displacement control. Schematic illustration of FSLW process has already been provided in Fig. 1. Fig.

2 shows an actual FSLW experiment. A Lowstir™ device, which is also shown in Fig. 2, was used in each FSLW experiment to monitor the downforce. Al 6060-T5 (300x100x6mm) alloy placed on top of the and pure Cu (300x100x2mm) work pieces were FSL welded. A sufficiently thick top plate is used to avoid fracture at the HAZ during tensile shear testing, and to instead cause fracture along the Al-Cu interface. A major series of experiments were conducted with 1400 rpm, (and 710 rpm is only used to demonstrate the difference in temperature at SZ, Fig 5) as a rotational speed (ω), 60mm/min as a traverse speed (v), 3 degrees of tilt angle (Θ) and tool pin penetration $D_p = 0$ mm and $D_p = 0.4$ mm respectively from the top surface of the bottom plate (Fig.3). Tools were made using H13 tool steel and the left-hand threads of the pins were made with a 1 mm pitch and a 0.6 mm actual depth. The diameter of the concave shoulder was 18 mm and the pin outside diameter was 6 mm. K-type thermocouple was used to measure the FSLW interface temperature.

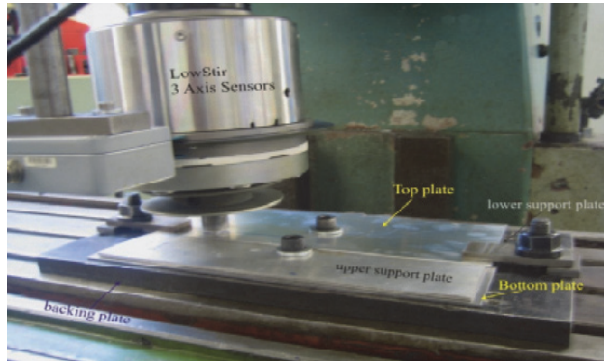


Fig. 2. FSLW using a FV200 milling machine with a Lowstir™ force measuring device

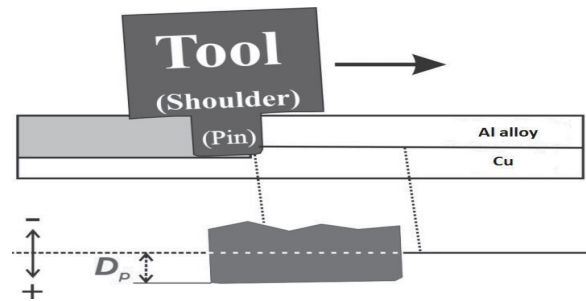


Fig. 3. Schematic illustration of tool positioning during FSLW showing pin penetration depth

Tensile-shear testing of FS lap welds has been the major method used for evaluating strength of FSL welds in literature. Test samples, 16 mm wide, perpendicular to the welding direction were machined from the welded plates. Fig. 4 illustrates the positioning of a sample together with supporting pieces. Samples were tested at a constant crosshead displacement rate of 3 mm/min using a 50 KN Tinus Olsen tensile testing machine, with a 50-mm extensometer attached. The strength of a lap sample cannot be expressed using the normal load/area, as the stress distribution along the joint area during tensile-shear test is highly uneven. Instead, maximum failure load in a test divided by the width of the sample, σ_{Lap} , is taken as strength

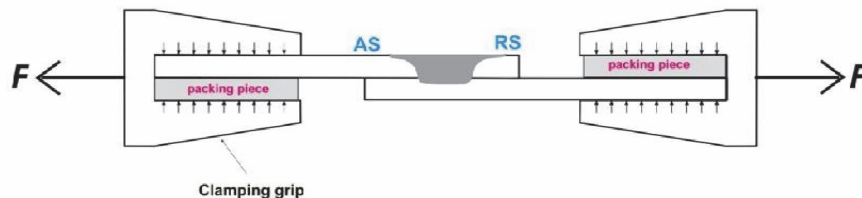


Fig. 4. Schematic illustration of tensile-shear testing

3. Results and discussion

3.1. Temperature measurement

To justify FSW is solid state welding process, (no melting of base metals). K-type thermocouple was placed at Al-Cu interface to monitor the temperature. Traces of temperature at stir zone (SZ) of these welds, during FSLW, are also presented in Fig 5. In each trace, there are disturbances in the peak

temperature region because the thermocouple was pushed slightly by the lower stir flow as the pin approached the thermocouple. The weld made using $\omega=1400$ rpm has obtained higher peak temperature ($T_{sz}=520^{\circ}\text{C}$) and spent longer time at the elevated temperatures, compared to the weld made using $\omega=710$ rpm (with $T_{sz}=445^{\circ}\text{C}$).

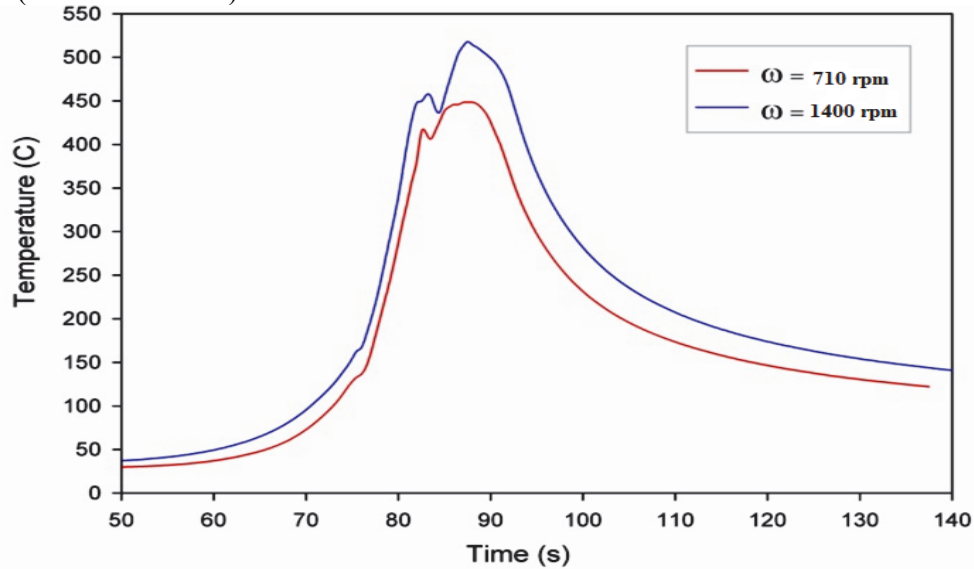


Fig. 5. Measured temperature at SZ of welds made using $\omega=1400$ rpm and $\omega=710$ rpm with $v=60\text{mm/min}$

3.2 Microhardness distribution in stir zone

As the larger grains have less grain boundaries hence they would impose less restriction to the dislocation movement, resulting in lower hardness and local strength. Therefore, the SZ exhibited the lowest hardness, compare to the other region, as it had the largest grains hardness of SZ for the weld made using $\omega=1400$ rpm is considerably lower than that of the weld made using $\omega=710$ rpm (Fig. 6). This is due to difference in grain size produced at SZ of these welds, as shown in Fig 7. The grains in the weld made using $\omega=1400$ rpm is considerably larger than the grains in the weld made using $\omega=710$ rpm. Traces of temperature at SZ of these welds, during FSLW, are also presented in Fig5. Consequently, the recrystallized grains at SZ of the weld made using $\omega=1400$ rpm could grow more, resulting in larger grains with subsequent reduced hardness.

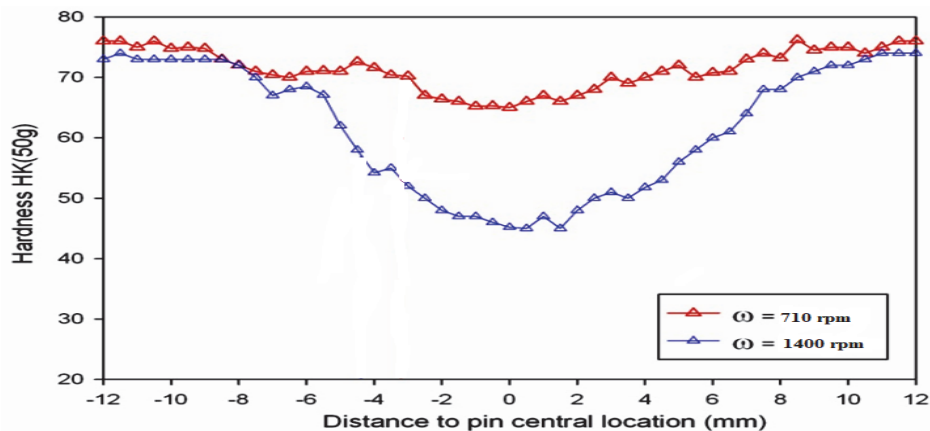


Fig. 6. Knoop hardness distribution (transverse to welding direction) measured for the two welds made using $\omega=1400$ rpm, 710 rpm and $v=60\text{mm/min}$

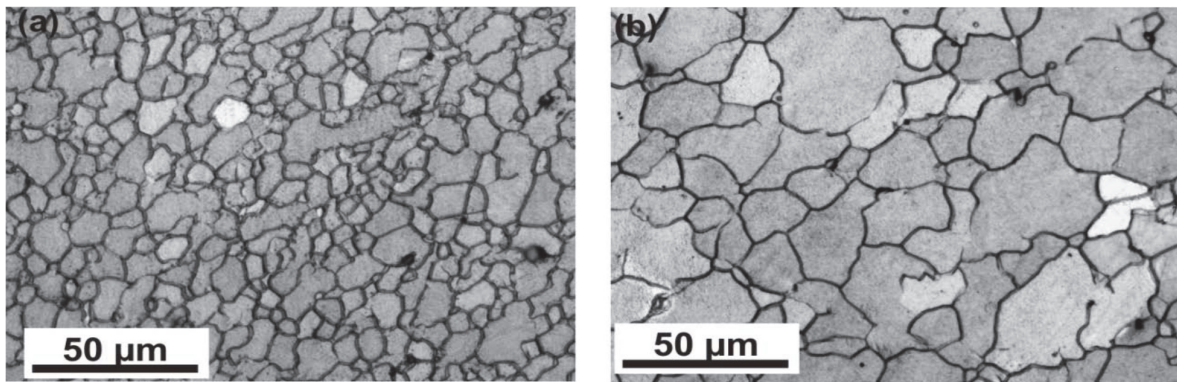


Fig. 7. Microstructure of SZ for the welds made using $v = 60$ mm/min: (a) $\omega = 710$ rpm and (b) $\omega = 1400$ rpm

3.3 Microstructure analysis

Three selected samples are shown here to illustrate the importance of interface microstructures and based on this illustration a suggestion of FSLW control for maximum strength can then be made. Fig. 8(a) is the first example where no intermetallic compound layer (IMC) were formed for $Dp \approx 0$. It should be noted that there is no research work available in literature for this condition especially for Al-Cu FSLW. The reason for not forming any intermetallic layer at the Al-Cu weld interface may be because copper has conducted heat faster, since copper has higher thermal conductivity, but for the similar FSLW conditions (pin penetration, $Dp \approx 0$) for Al-Steel FSLW, a continuous and thin intermetallic layer has been reported (Shubhavardhan & Surendran 2018). This is just to compare the effect of FSLW pin penetration (Dp) on different large ΔT Melting couple, however, FSLW of Al-steel and Al-copper is totally different, cannot compare the results), with maximum value of σ_{Lap} . When $Dp \approx 0.4$ as shown in in fig. 8(b), a thin and continuous interface intermetallic layer (up to $3\mu\text{m}$ in thickness) is observed. When the pin penetration is further increased a non-uniform, irregular intermix MSZ can be observed which is shown in fig 8(c). The area of MSZ largely corresponds to the area of the pin penetrated copper and this zone is a mixture of Al-Cu intermetallic thin pieces embedded in the recrystallized Cu grains.

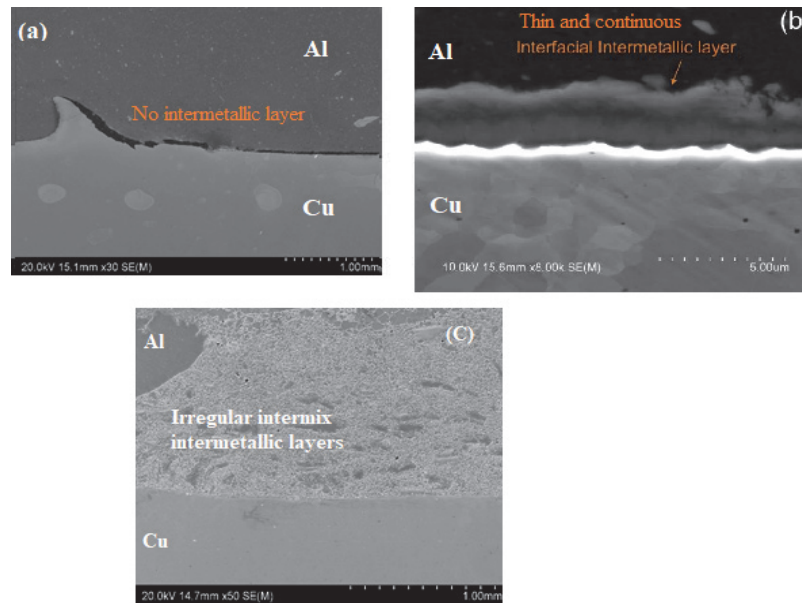


Fig. 8. Cross sectional view of an Al-Cu FSL weld made with $\omega = 1,400$ rpm, $v = 60$ mm/min, (a) $Dp \approx 0$ with no intermetallic layer formed at the interface, (b) $Dp \approx 0.4$ mm thin and continuous intermetallic layer formed, and (c) $Dp > 0.4$ mm displaying irregular intermix intermetallic layer (MSZ)

In Fig. 8(b) as mentioned earlier a thin and continuous interface intermetallic layer can be observed. A metallurgical bond between Al and Cu is established due to the diffusion of Cu and Al, and thus a slight pin penetration $D_p \approx 0.4$, (referring to Fig. 3) is commonly believed to be the condition for a good weld strength. Naturally, no intermetallic layer or a MSZ cannot form and if $D_p < 0$. However, FS tool can be position controlled so that $D_p \approx 0$. In this case, although there can still be an absence of intermetallic layer and MSZ, but it is totally different in case of Al-steel FSLW. Shubhavardhan and Surendran (2018), because as has already explained the thermal conductivity of steel is lesser than copper, the reason could be steel conducted heat far slower than the copper, forming a thin and continuous intermetallic layer at Al-Steel FSLW interface for $D_p \approx 0$. A thin Al-Cu interface intermetallic compound layer can form when pin penetration D_p is 0.4mm, metallurgical bonding the top and bottom plates together, as demonstrated by an example shown in Fig. 9.

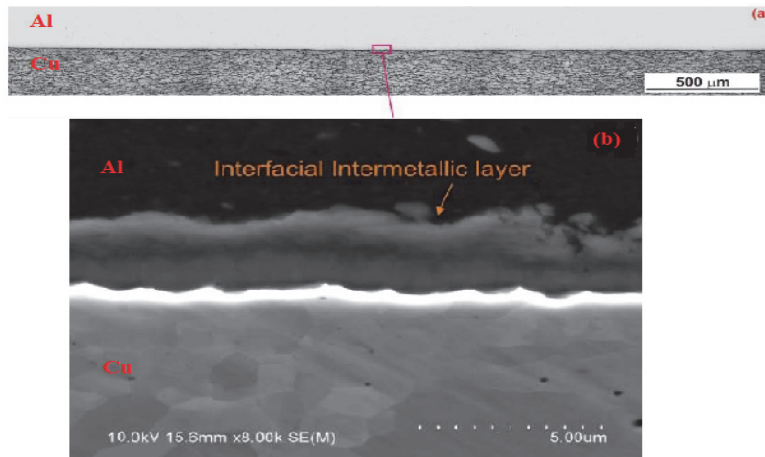
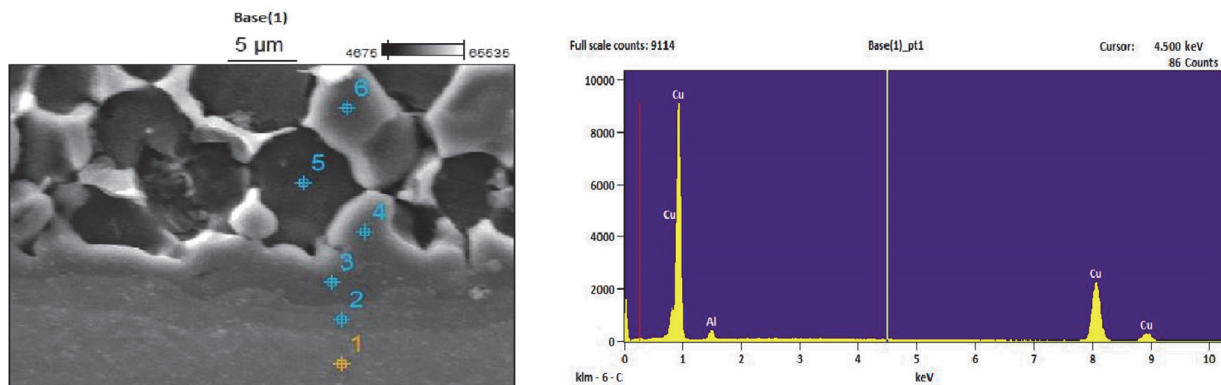
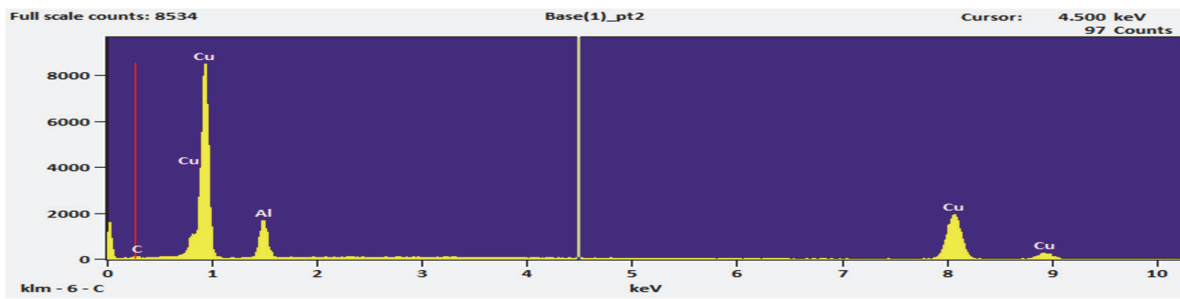
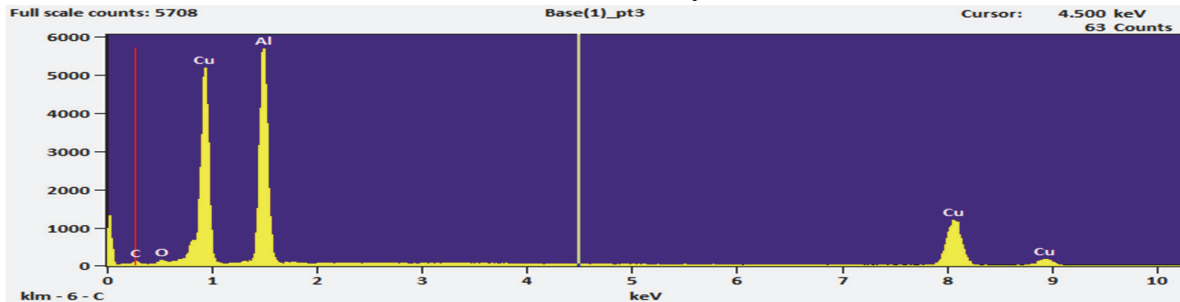
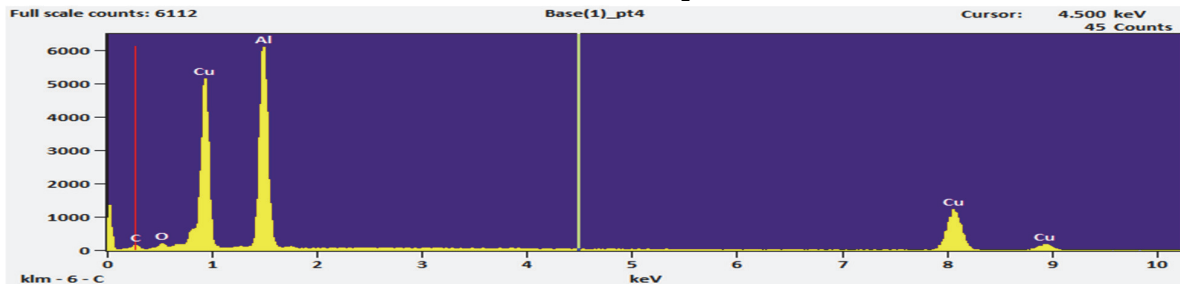
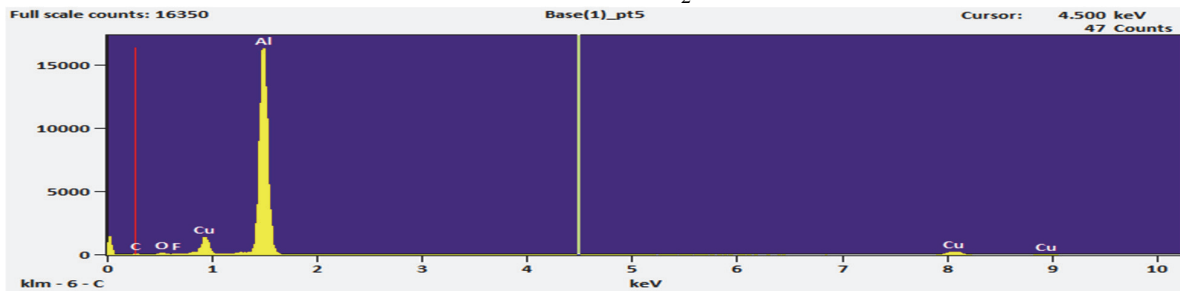


Fig. 9. Cross sectional view of an Al-Cu weld made with $\omega = 1,400$ rpm, $v = 60$ mm/min and $D_p \approx 0.4$ mm, (a) optical macrograph and (b) SEM micrograph of Al-Cu interface displaying no defect but a continuous thin interface layer

Furthermore, formation of intermetallic layers at the Al-Cu interface was further investigated using EDS spot analysis. Typical EDS spectra of intermetallic layers at the Al/Cu interface and inside the stir zone for $D_p \approx 0.4$ mm is presented in Fig 10. At point 1 we can notice presence of copper rich phase, and Al rich phase at point 5, point 2 indicate that the thin layer at Al-Cu interface is mainly Al_4Cu_9 intermetallic, according to Al-Cu phase diagram, On the other hand, point 3 and 4 indicate presence of AlCu intermetallic layer, the chemical composition of 61.8at%Al and 38.2at%Cu in Fig 10 at point 6 may indicate that the thin layer within the stir zone is likely to be Al_2Cu intermetallic phase. Some of the observed intermetallic layers here were also found in literature (Elrefaey et al; 2004, Xue et al; 2011a,b). However, due to the analytical spot size being large in SEM/EDS hence assigning the structure of Al_2Cu , AlCu or Al_4Cu_9 to the small size intermetallic layers is not very reliable.



Point 2; $\text{Al}_4\text{Cu}_9(\gamma_1)$ Point 3; $\text{AlCu}(\eta_2)$ Point 4; $\text{AlCu}(\eta_2)$ 

Point 5; Al

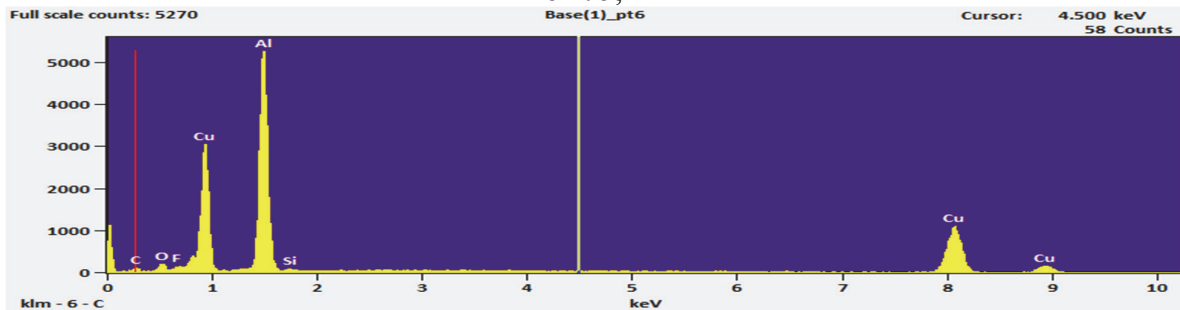
Point 6; $\text{Al}_2\text{Cu}(\theta)$

Fig. 10. SEM micrograph showing the intermetallic layers at Al/Cu interface, EDS spectra of intermetallic layer at different locations in stir zone are also shown

3.4 Al-Cu Fracture strength

Before discussing the effect of D_p on fracture behavior, the strain measurement should be discussed first. Unlike traditional tensile testing where the sample is elongated axially, in a tensile-shear test, the extension is slightly axially off and there is a degree of local rotation during testing if sufficient plasticity of the sample allows. Thus, the axial strain measurement by the extensometer is slightly distorted due to the slightly local twisting/bending. Furthermore, particularly in the initial stage of elongation (largely within the linear range), the extension values measured by the extensometer were slightly unstable. Thus, determined strain values are not highly accurate but the use of them should be adequate for indicating plasticity. Fig 11 shows selected tensile-shear curves. For the penetrated sample more than 0.4mm, there is a significant amount of fracture energy (E_f), represented by the area under the curve. The weld strength was 302 N/mm, which is obviously much higher than that of $D_p \approx 0$ (0 N/mm, which is not discussed furthermore) but is considerably lower than that of Al-Cu FSL welds (> 450 N/mm), with $D_p \approx 0.4$ mm. The weld strength of 302 N/mm is higher than the values of 268 N/mm which is the maximum value obtained for samples using a pin penetration (P Xue et al;2011). In this latter study, when a weld is free of macro- defects the strength equivalent value is close to that maximum value, regardless of what the FS speeds condition.

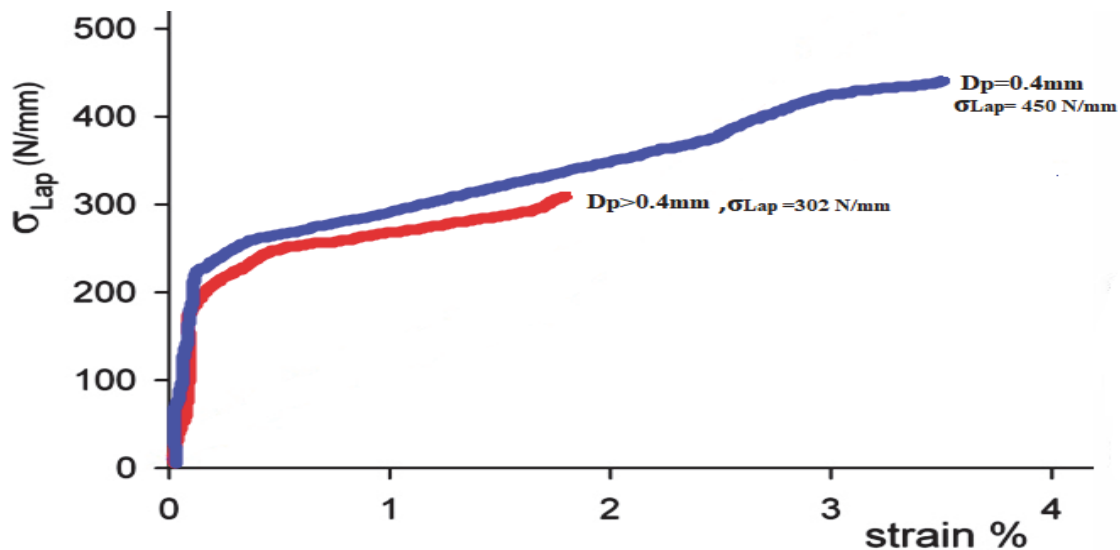


Fig. 11. Tensile-shear curves of two samples of welds made with $\omega = 1,400$ rpm, $v = 60$ mm/min and D_p values as indicated

When $D_p \approx 0.4$ and an interface intermetallic layer was established without MSZ, fracture strength (450 N/mm) is considerably higher than that for the sample with MSZ (302 N/mm, fractured at SZ). The large deformation is accompanied by a corresponding amount of work hardening, as is indicative in the tensile-shear curve in Fig. 11, and thus by a high σ_{Lap} value of 475 N/mm. It is clear by viewing the tested samples in Fig. 12. For the pin penetrated sample $D_p > 0.4$ mm (Fig 12a), the sample having been slightly bent is evident. On the other hand, for the $D_p \approx 0.4$ mm sample (Fig 12b), a large amount of local deformation and bending before the final fracture at SZ is clearly the feature. The presence of thin and continuous intermetallic layer in the $D_p \approx 0.4$ mm sample means a different fracture behavior. The large amounts of deformation and fracture energy for this sample means that the thin interface layer is not brittle under tensile-shear condition. From the present results, it can be suggested that careful positioning control for Al-Cu FSL welds is a mean for the optimal weld strength to be obtained.



Fig.12. Tensile-shear tested samples of welds made with $\omega = 1,400$ rpm, $v = 60$ mm/min and (a) $D_p > 0.4$ mm and (b) $D_p \approx 0.4$ mm

4. Conclusion

For Al-Cu FSL welds, fracture strength was found to be very sensitive to pin positioning during FSLW. When $D_p \approx 0.4$ mm, a single continuous intermetallic layer formed along the interface; and thus, continuous metallurgical bonding established. The joint produced by this pin penetrating condition (with a single continuous intermetallic at interface) displayed a higher σ_{Lap} value (450 N/mm) which was $\sim 49\%$ increase in σ_{Lap} in comparison to the case of $D_p > 0.4$ mm condition (with the mixed interface region). The condition of $D_p > 0.4$ mm did not insure a continuous intermetallic layer and instead discontinuous intermetallic outbursts (non-continuous metallurgical bond) formed at the interface, resulting from the early stage of intermetallic growth, formed at the joint interface. Once the pin sufficiently penetrates to copper ($D_p > 0.4$ mm), the interface region was consisted of intermix and irregular layers of intermetallic and recrystallized Cu grains form. The value of σ_{lap} (≈ 302 N/mm) in pin penetrating condition, although D_p differ for different samples, indicates that σ_{Lap} is not very sensitive to the size of the interface region (with intermix and irregular intermetallic layers), once it forms. Also, value of σ_{lap} (≈ 302 N/mm, fractured at SZ) for the pin penetrated welds is itself higher than the maximum σ_{lap} value (268 N/mm, fractured at the SZ or interface) reported in literature when pin penetrating condition used. In tensile shear loading of $D_p > 0.4$ mm samples (with the mixed interface region) failure occurred through crack propagation along the intermetallic layers embedded inside the penetrated region, resulting in a brittle fracture. However, for the sample made using $D_p \approx 0.4$ mm condition (with a single continuous intermetallic layer at interface), a ductile fracture was dominant with plastic deformation preceding failure mostly in aluminum adjacent to and on top of the interfacial intermetallic layer. Therefore, these results indicate that the notion of the presence of intermetallic layers embrittling the joint, is scientifically incorrect and a joint interface with single intermetallic layer can be highly shear fracture resistant.

References

- Abdollah-Zadeh, A., Saeid, T., & Sazgari, B. (2008). Microstructural and mechanical properties of friction stir welded aluminum/copper lap joints. *Journal of alloys and Compounds*, 460(1-2), 535-538.
- Akbari, M., & Behnagh, R. A. (2012). Dissimilar friction-stir lap joining of 5083 aluminum alloy to CuZn34 brass. *Metallurgical and Materials Transactions B*, 43(5), 1177-1186.
- Akbari, M., Aliha, M. R. M., Keshavarz, S. M. E., & Bonyadi, A. (2016). Effect of tool parameters on mechanical properties, temperature, and force generation during FSW. *Proceedings of the Institution*

- of *Mechanical Engineers, Part L: Journal of Materials: Design and Applications*, 1464420716681591.
- Aliha, M. R. M., Kalantari, M. H., Ghoreishi, S. M. N., Torabi, A. R., & Etesam, S. (2019). Mixed mode I/II crack growth investigation for bi-metal FSW aluminum alloy AA7075-T6/pure copper joints. *Theoretical and Applied Fracture Mechanics*, 102243.
- Aliha, M. R. M., Shahheidari, M., Bisadi, M., Akbari, M., & Hossain, S. (2016). Mechanical and metallurgical properties of dissimilar AA6061-T6 and AA7277-T6 joint made by FSW technique. *The International Journal of Advanced Manufacturing Technology*, 86(9-12), 2551-2565.
- Carlone, P., Astarita, A., Palazzo, G. S., Paradiso, V., & Squillace, A. (2015). Microstructural aspects in Al-Cu dissimilar joining by FSW. *The International Journal of Advanced Manufacturing Technology*, 79(5-8), 1109-1116.
- DebRoy, T., & Bhadeshia, H. K. D. H. (2010). Friction stir welding of dissimilar alloys—a perspective. *Science and Technology of Welding and Joining*, 15(4), 266-270.
- Elrefaey, A., Takahashi, M., & Ikeuchi, K. (2004). Microstructure of aluminum/copper lap joint by friction stir welding and its performance. *Journal of High Temperature Society*, 30(5), 286-292.
- Elrefaey, A., Takahashi, M., & Ikeuchi, K. (2005). Preliminary investigation of friction stir welding aluminium/copper lap joints. *Welding in the World*, 49(3-4), 93-101.
- Esmaili, A., Givi, M. B., & Rajani, H. Z. (2011a). A metallurgical and mechanical study on dissimilar Friction Stir welding of aluminum 1050 to brass (CuZn30). *Materials Science and Engineering: A*, 528(22-23), 7093-7102.
- Esmaili, A., Rajani, H. Z., Sharbati, M., Givi, M. B., & Shamanian, M. (2011b). The role of rotation speed on intermetallic compounds formation and mechanical behavior of friction stir welded brass/aluminum 1050 couple. *Intermetallics*, 19(11), 1711-1719.
- Firouzdar, V., & Kou, S. (2012). Al-to-Cu friction stir lap welding. *Metallurgical and Materials Transactions A*, 43(1), 303-315.
- Galvao, I., Oliveira, J. C., Loureiro, A., & Rodrigues, D. M. (2011). Formation and distribution of brittle structures in friction stir welding of aluminium and copper: influence of process parameters. *Science and Technology of Welding and Joining*, 16(8), 681-689.
- Galvão, I., Oliveira, J. C., Loureiro, A., & Rodrigues, D. M. (2012b). Formation and distribution of brittle structures in friction stir welding of aluminium and copper: Influence of shoulder geometry. *Intermetallics*, 22, 122-128.
- Galvao, I., Verdera, D., Gestó, D., Loureiro, A., & Rodrigues, D. M. (2012a). Analysing the challenge of aluminum to copper FSW. In *Proceedings of 9th International Symposium on Friction Stir Welding, Huntsville, Alabama, US*.
- Genevois, C., Girard, M., Huneau, B., Sauvage, X., & Racineux, G. (2011). Interfacial reaction during friction stir welding of Al and Cu. *Metallurgical and Materials Transactions A*, 42(8), 2290.
- Kumbhar, N. T., & Bhanumurthy, K. (2012). Friction stir welding of Al 5052 with Al 6061 alloys. *Journal of metallurgy*, 2012.
- Liu, H. J., Shen, J. J., Zhou, L., Zhao, Y. Q., Liu, C., & Kuang, L. Y. (2011). Microstructural characterisation and mechanical properties of friction stir welded joints of aluminium alloy to copper. *Science and Technology of Welding and Joining*, 16(1), 92-98.
- Lohwasser, D., & Chen, Z. (Eds.). (2009). *Friction stir welding: From basics to applications*. Elsevier.
- Lomolino, S., Tovo, R., & Dos Santos, J. (2005). On the fatigue behaviour and design curves of friction stir butt-welded Al alloys. *International Journal of Fatigue*, 27(3), 305-316.
- Mishra, R. S., & Ma, Z. Y. (2005). Friction stir welding and processing. *Materials science and engineering: R: reports*, 50(1-2), 1-78.
- Mishra, R. S., & Mahoney, M. W. (2007). Friction stir welding and processing, ASM International. *Material Park, Ohio, The Materials Information Society*.
- Mohammad Aliha, M. R., Fotouhi, Y., & Berto, F. (2018). Experimental notched fracture resistance study for the interface of Al-Cu bimetal joints welded by friction stir welding. *Proceedings of the Institution of Mechanical Engineers, Part B: Journal of Engineering Manufacture*, 232(12), 2192-2200.

- Murr, L. E. (2010). A review of FSW research on dissimilar metal and alloy systems. *Journal of Materials Engineering and Performance*, 19(8), 1071-1089.
- Nandan, R., DebRoy, T., & Bhadeshia, H. K. D. H. (2008). Recent advances in friction-stir welding—process, weldment structure and properties. *Progress in materials science*, 53(6), 980-1023.
- Ouyang, J., Yarrapareddy, E., & Kovacevic, R. (2006). Microstructural evolution in the friction stir welded 6061 aluminum alloy (T6-temper condition) to copper. *Journal of Materials Processing Technology*, 172(1), 110-122.
- Pao, P. S., Gill, S. J., Feng, C. R., & Sankaran, K. K. (2001). Corrosion–fatigue crack growth in friction stir welded Al 7050. *Scripta Materialia*, 45(5), 605-612.
- Rai, R., De, A., Bhadeshia, H. K. D. H., & DebRoy, T. (2011). friction stir welding tools. *Science and Technology of welding and Joining*, 16(4), 325-342.
- Saeid, T., Abdollah-Zadeh, A., & Sazgari, B. (2010). Weldability and mechanical properties of dissimilar aluminum–copper lap joints made by friction stir welding. *Journal of Alloys and Compounds*, 490(1-2), 652-655.
- Satya Narayana Gupta, M., Balunaik, B., & Murti, K. G. K. (2012). Effect of Tool Geometry on Joint Properties of Friction Stir Welded Al/Cu Bimetallic Lap Joints. *IUP Journal of Mechanical Engineering*, 5(1).
- Sharma, N., Siddiquee, A. N., Khan, Z. A., & Mohammed, M. T. (2018). Material stirring during FSW of Al–Cu: Effect of pin profile. *Materials and Manufacturing Processes*, 33(7), 786-794.
- Shubhavardhan, R., & Surendran, S. (2018). Microstructure and fracture behavior of friction stir lap welding of dissimilar metals. *Engineering Solid Mechanics*, 6(1), 1-10.
- Sun, Y. F., Fujii, H., Takaki, N., & Okitsu, Y. (2013). Microstructure and mechanical properties of dissimilar Al alloy/steel joints prepared by a flat spot friction stir welding technique. *Materials & design*, 47, 350-357.
- Thomas, W. M., Nicholas, E. D., Needham, J. C., Murch, M. G., Temple Smith, P., & Dawes, C. J. (1993). *Improvements Relating to Friction Welding*. International Patent Application No (Vol. 1, p. 6). PCT/GB92/02203 Publication No. WO19930109935.
- Threadgill, P. L., Leonard, A. J., Shercliff, H. R., & Withers, P. J. (2009). Friction stir welding of aluminium alloys. *International Materials Reviews*, 54(2), 49-93.
- Torabi, A. R., Kalantari, M. H., & Aliha, M. R. M. (2018). Fracture analysis of dissimilar Al–Al friction stir welded joints under tensile/shear loading. *Fatigue & Fracture of Engineering Materials & Structures*, 41(9), 2040-2053.
- Wang, X., Pan, Y., & Lados, D. A. (2018). Friction stir welding of dissimilar Al/Al and Al/non-Al alloys: a review. *Metallurgical and Materials Transactions B*, 49(4), 2097-2117.
- Xue, P., Ni, D. R., Wang, D., Xiao, B. L., & Ma, Z. Y. (2011b). Effect of friction stir welding parameters on the microstructure and mechanical properties of the dissimilar Al–Cu joints. *Materials science and engineering: A*, 528(13-14), 4683-4689.
- Xue, P., Xiao, B. L., Ni, D. R., & Ma, Z. Y. (2010). Enhanced mechanical properties of friction stir welded dissimilar Al–Cu joint by intermetallic compounds. *Materials science and engineering: A*, 527(21-22), 5723-5727.
- Xue, P., Xiao, B. L., Wang, D., & Ma, Z. Y. (2011a). Achieving high property friction stir welded aluminium/copper lap joint at low heat input. *Science and technology of welding and Joining*, 16(8), 657-661.
- Zettler, R., Da Silva, A. A. M., Rodrigues, S., Blanco, A., & Dos Santos, J. F. (2006). Dissimilar Al to Mg alloy friction stir welds. *Advanced Engineering Materials*, 8(5), 415-421.
- Zhang, W., Shen, Y., Yan, Y., Guo, R., Guan, W., & Guo, G. (2018). Microstructure characterization and mechanical behavior of dissimilar friction stir welded Al/Cu couple with different joint configurations. *The International Journal of Advanced Manufacturing Technology*, 94(1-4), 1021-1030.



© 2019 by the authors; licensee Growing Science, Canada. This is an open access article distributed under the terms and conditions of the Creative Commons Attribution (CC-BY) license (<http://creativecommons.org/licenses/by/4.0/>).